IN-SITU DISCOVERY OF PRESOLAR SILICATES FROM PRIMITIVE CHONDRITES. K. Nagashima[1], A. N. Krot[2], and H. Yurimoto[1], [1]Department of Earth and Planetary Sciences, Tokyo Institute of Technology, Ookayama 2-12-1, Meguro, Tokyo 152-8551, Japan (kazu@geo.titech.ac.jp), [2]Hawai'i Institute of Geophysics and Planetology, School of Ocean and Earth Science and Technology, University of Hawai'i at Manoa, Honolulu, HI 96822, USA.

Introduction: It is known from ISO spectra that crystalline forsterite, enstatite, and amorphous silicates are the major silicate species in circumstellar disks around young stars and in outflows from red giants [1]. Although recently presolar silicate grains were identified in IDPs [2], presolar silicates have not been identified in meteorites so far even though several research to find presolar silicates were conducted [3-4]. Here we employed *in-situ* large-scale surveys of presolar grains in primitive chondrites using ion microscopy.

Experimental: The samples used in this study are polished thin sections from the Acfer 094 unique, type3 carbonaceous chondrite and the NWA 530 CR2 chondrite. Petrologic and mineralogical studies were made using a scanning electron microscope (JEOL JSM-5310LV) equipped with an energy dispersive X-ray spectrometer (Oxford LINK-ISIS). This system was also used to obtain X-ray elemental maps.

Isotope images were obtained by the TiTech isotope microscope (Cameca ims-1270 + SCAPS [5]). The analytical techniques for isotope images generally followed those described in [6]. The size of an ion image corresponds to 70 x 70 µm on the sample. The width of the energy bandpass was set to 20 eV in order to improve lateral resolution of the image. The exit slit was narrowed enough to eliminate the contribution of interference ions to the isotopic images.

The typical sequence for acquiring secondary ion images was $^{27}Al^-$, $^{28}Si^-$, $^{29}Si^-$, $^{28}Si^-$, $^{30}Si^-$, $^{28}Si^-$, $^{16}O^-$, $^{18}O^-$, $^{16}O^-$, $^{17}O^-$, $^{16}O^-$, $^{12}C^-$, $^{13}O^-$, and $^{12}C^-$ for one analysis. Total integration time for one analysis was ~1.5 hour. The sputtering depth was less than 100 nm. The digital image processing using a moving-average with 5 x 5 pixels was applied to simple secondary ion ratio image in order to reduce the statistical error. For oxygen isotope images, the average values of relative secondary ion ratios from the matrix areas in the images were normalized to SMOW scale using literature values [7-8].

Typical errors for $\delta^{17}O$ and $\delta^{18}O$ images were estimated by the random isotopic variation appeared in the matrix, indicating 40 ‰ and 15 ‰ (3σ), respectively and shown in Fig. 1 as error ellipses. Such high precision allows to recognize micro-scale refractory inclusions in δO images if exist (e.g. most mottling appeared in Fig. 2(a); an AOA fragment of lower-right in Fig. 2(b))

Results and discussion: 9 different matrix areas of Acfer 094 and of NWA 530 were analyzed. Total survey areas were about 44100 μm^2 for each chondrite. Candidates of presolar silicate grains are appeared as hotspots (warm or cold colors) in δO images, like spots indicated by arrows in the Fig. 2(a) and (b).

Since these measurements are performed *in-situ* and lateral resolution of the ion image is limited ~1µm, the isotopically anomalous values of hotspots are diluted extremely by contributions of surrounding isotopically solar matrix grains if grains at hotspots are equivalent to or smaller than the lateral resolution. Therefore, the peak values are adopted for the isotopic values of each hotspot correspond to lower limits. The errors are estimated by the isotopic variations at the peak tops in the δO images.

Each hotspot identified in δO images was plotted in three O isotope diagram. Selection criterion for considering presolar candidates is that these isotopic ratios are >2σ away from the 3σ ellipse of the distribution of the isotopically solar matrix. Using this criterion, 4 grains from Acfer 094 and 3 grains from NWA 530 are classified as presolar grains (Fig. 1). The O-isotopic compositions of these presolar grains fall within the range of values previously observed among meteoritic presolar oxide grains in meteorites [e.g. 9-10] and silicate grains in IDPs [2], and represent typical group 1 presolar grains. On the other hand, Si isotopic compositions of these grains calculated from Si isotope images seem to be solar compositions within analytical errors (~60 ‰ in 3σ).

Phase characterizations of these presolar grains were conducted by scanning electron microscopy with elemental mapping. All presolar grains shown in Fig. 1 are silicates or oxides because of intense secondary ion intensities of O and consisting of aggregations of these phases. Grain identification of a presolar grain, however, is not easy because typical grain sizes of matrix of these meteorites are 0.2 µm which are less than lateral resolution of the isotope images and X-ray elemental maps. Therefore we cannot remove ambiguity completely for the phase characterization.

Under these circumstances, the hotspot of Fig. 2(a) seems to be Mg-rich olivine of ~1 µm size (Fig.

3) based on the position matching and conformity in grain shape between images. One hot spot (not shown images) corresponds to corundum or hibonite with ~0.2 µm size because intense Al peak and slight depletions of Mg, Si and Fe abundances were observed at the location. On the other hand, X-ray elemental maps show no Al peaks and show high abundances of Si, Mg, and Fe at the locations of other five hotspots. The locations contain aggregates of ~0.2 µm sized silicate grains. These characteristics suggest that other five grains are silicates although grain identifications have been failed.

Grain densities of presolar silicates in Acfer 094 and NWA530 are roughly estimated to be ~70 /mm^2. Since grain size distribution of presolar silicates in this study is similar to those by [2], abundances of sub-micron sized presolar silicates are clearly lower than those of anhydrous cluster IDPs (~20000 /mm^2, [2]). If the lower abundances are due to aqueous and thermal alteration processes after accretion to the parent bodies, the similar size distribution of presolar silicates between the meteorites and the IDPs cannot be explained. Therefore this suggests that incorporation of presolar grains was smaller in chondrite forming region than in comet forming region or incorporation of materials produced in solar nebula were larger in chondrule forming region.

References: [1] Waters L. B. F. M. et al. (1996) *Astron. Astrophys*., **315**, L361. [2] Messenger S. et al. (2003) *Science*, **300**, 105. [3] Messenger S. and Bernatowicz T. J. (2000) *M&PS,* 35, A109. [4] Mostefaoui S. (2003) *M&PS,* 38, A5185. [5] Yurimoto H. et al. (2003) *Appl. Surf. Sci.,* **203-204**, 793. [6] Kunihiro T. et al. (2003) *GCA*, submitted. [7] Bicshoff A. et al. (1991) *Meteoritics* **26**, 318. [8] Clayton R. N. and Mayeda T. K. (1999) *GCA*, **63**, 2089. [9] Nittler L. R. et al. (1997) *ApJ*, **483**, 475. [10] Zinner E. et al. (2003) *GCA*, **67**, 5083.

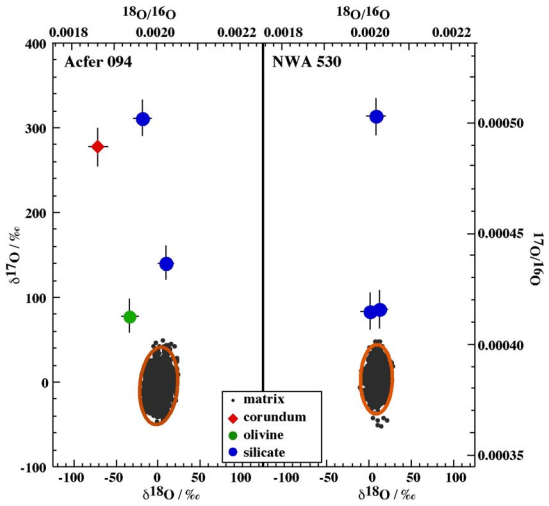

Figure 1: Oxygen isotopic ratios of presolar corundum, olivine, and unidentified silicate grains. Also shown are the isotopic ratios of isotopically solar matrix. Error ellipses around plots for the matrix have axes that are three times the standard deviation in the direction of the correlation line for the matrix and normal to it. Error bars for presolar grains denote 2σ.

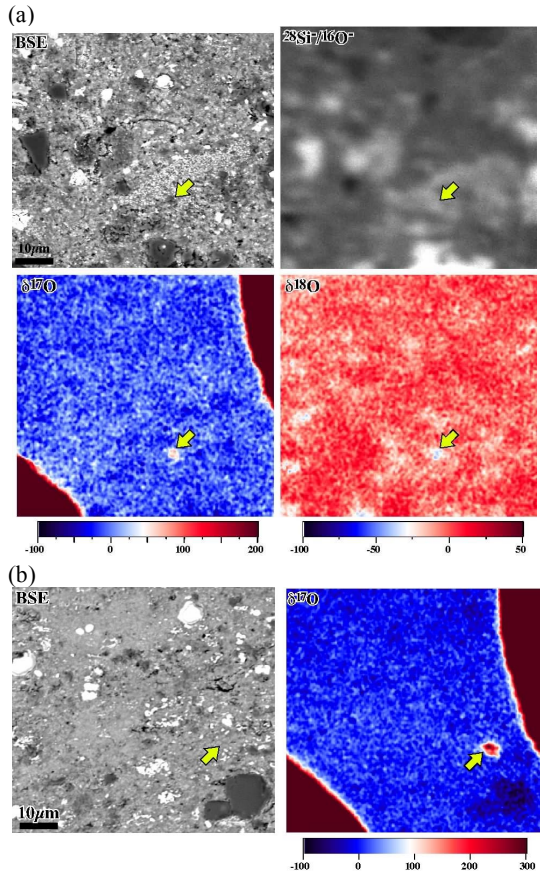

Figure 2. (a): Corresponding images among BSE, secondary ion ratio of ^{28}Si$^-$/^{16}O$^-$, and δ^{17}O and δ^{18}O of matrix in Acfer 094. (b): Corresponding images between BSE and δ^{17}O of matrix in NWA 530. Yellow arrows indicate locations of presolar grains. Reddish brown areas of upper right and lower left corners of δ^{17}O images are blurred by ^{16}OH$^-$ interference.

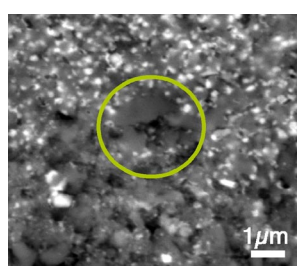

Figure 3: A magnified BSE image of matrix from Acfer 094. The yellow circle shows the location of a ^{17}O-rich Mg-rich olivine grain arrowed in Fig. 1(a).